Original Article

Insulin and Inositol 1,4,5-Trisphosphate Trigger Abnormal Cytosolic Ca^{2+} Transients and Reveal Mitochondrial Ca^{2+} Handling Defects in Cardiomyocytes of *ob/ob* Mice

Jérémy Fauconnier, Johanna T. Lanner, Shi-Jin Zhang, Pasi Tavi, Joseph D. Bruton, Abram Katz, and Håkan Westerblad

Obesity, insulin resistance, and type 2 diabetes are leading causes of heart failure, and defective cellular Ca^{2+} handling seems to be a fundamental problem in diabetes. Therefore, we studied the effect of insulin on Ca^{2+} homeostasis in normal, freshly isolated mouse ventricular cardiomyocytes and whether Ca^{2+} handling was changed in an animal model of obesity and type 2 diabetes, *ob/ob* mice. Electrically evoked Ca^{2+} transients were smaller and slower in *ob/ob* compared with wild-type cardiomyocytes. Application of insulin (6 or 60 nmol/l) increased the amplitude of Ca^{2+} transients in wild-type cells by ~30%, whereas it broadened the transients and triggered extra Ca^{2+} transients in *ob/ob* cells. The effects of insulin in *ob/ob* cells could be reproduced by application of a membrane-permeant inositol trisphosphate (IP_3) analog and blocked by a frequently used IP_3 receptor inhibitor, 2-aminoethoxydiphenyl borate. In *ob/ob* cardiomyocytes, insulin increased the IP_3 concentration and mitochondrial Ca^{2+} handling was impaired. In conclusion, we propose a model where insulin increases IP_3 in *ob/ob* cardiomyocytes, which prolongs the electrically evoked Ca^{2+} release. This, together with an impaired mitochondrial Ca^{2+} handling, results in insulin-mediated extra Ca^{2+} transients in *ob/ob* cardiomyocytes that may predispose for arrhythmias in vivo. *Diabetes* 54:2375–2381, 2005

Obesity and type 2 diabetes are leading causes of coronary heart disease and heart failure (1–4), and clinical and experimental studies have shown that diabetes is associated with altered cardiac function independent of vascular complications (5,6). Defective cellular Ca^{2+} handling is a fundamental problem in diabetes (7). For instance, diabetic cardiomyopathy is characterized by reduced levels of Ca^{2+}-handling proteins and sarcoplasmic reticulum dysfunction leading to smaller and slower cytoplasmic Ca^{2+} transients (8).

Peripheral insulin resistance and hyperinsulinemia are hallmarks of type 2 diabetes and obesity. Insulin regulates various physiological processes in the heart including energy metabolism, contractility, protein expression, and ion transport (9). All insulin-mediated biological responses are consequences of the interaction between the insulin receptor, which belongs to the tyrosine kinase receptor family, and a complex array of downstream proteins (10,11). One central and early event in insulin signaling is the activation of phosphoinositide 3-kinase (PI3K), although insulin may also activate intracellular targets (e.g., MAP kinases) independent of PI3K activation. One tentative downstream target of PI3K is phospholipase C (PLC)-γ (12–14). Activation of PLC-γ induces hydrolysis of phosphatidylinositol-bisphosphate (4,5) to inositol 1,4,5-trisphosphate (IP_3) and diacylglycerol (15). IP_3 acts as a second messenger that mobilizes Ca^{2+} from intracellular stores via activation of specific IP_3 receptors, whereas a major function of diacylglycerol is to activate protein kinase C (15). Insulin may also interfere with other modes of IP_3 signaling in cardiomyocytes and, in this way, indirectly increase the IP_3 concentration (16). Several studies have shown that IP_3 can induce cardiac arrhythmias (17–19), and hence alterations in IP_3 signaling might be involved in diabetic cardiomyopathy. Elevated IP_3 has also been linked to an increased Ca^{2+} influx into cells via a process named capacitive calcium entry (CCE) (20). Recently, CCE was shown to be important for the sustained elevation of cytoplasmic Ca^{2+} and hence, Ca^{2+}-dependent cardiac remodelling after agonist stimulation of cultured

---

From the Department of Physiology and Pharmacology, Karolinska Institutet, Stockholm, Sweden.

Address correspondence and reprint requests to Håkan Westerblad, Department of Physiology and Pharmacology, Karolinska Institutet, SE-171 77 Stockholm, Sweden. E-mail: hakan.westerblad@fyfa.ki.se.

Received for publication 14 January 2005 and accepted in revised form 5 May 2005.

A.K. and H.W. have received grant support from Biovitrum Partner.

2-APB, 2-aminoethoxydiphenyl borate; CCE, capacitive calcium entry; IP_3, inositol 1,4,5-trisphosphate; PI3K, phosphoinositide 3-kinase; PLC, phospholipase C.

neonatal rat ventricular myocytes (21). Furthermore, PLC-mediated CCE in cardiomyocytes was decreased by hyperglycemia-induced stimulation of the hexosamine pathway (22,23).

Diabetes is associated with mitochondrial dysfunction, increased production of reactive oxygen species (24), and decreased mitochondrial Ca^{2+} loading capacity (25,26). In the heart, altered mitochondrial Ca^{2+} uptake could have a deleterious effect on global Ca^{2+} homeostasis because mitochondria may act as a fixed spatial buffering system directly interacting with sarcoplasmic reticulum Ca^{2+} release (26).

The aim of the present study was to characterize insulin effects on Ca^{2+} homeostasis in normal mouse ventricular cardiomyocytes and to determine whether Ca^{2+} handling was changed in an animal model of type 2 diabetes, i.e., obese leptin-deficient *ob/ob* mice (27). We specifically focus on the role of IP$_3$ and mitochondrial Ca^{2+} uptake. The results show marked differences between control and *ob/ob* cardiomyocytes that will increase the understanding of mechanisms underlying diabetic cardiomyopathy.

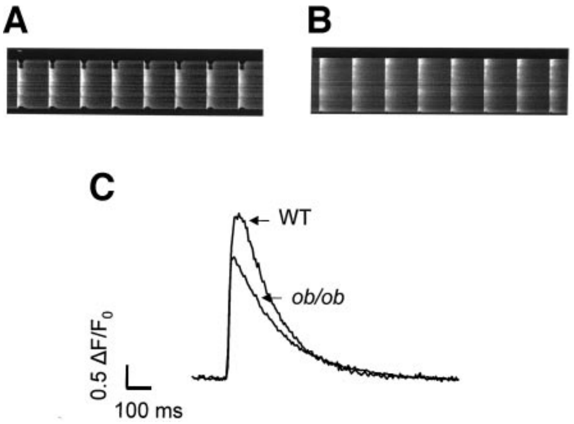

FIG. 1. Electrically evoked Ca^{2+} transients in ventricular cardiomyocytes from wild-type and *ob/ob* mice. Confocal line-scan images from a wild-type (*A*) and an *ob/ob* (*B*) cell stimulated at 1 Hz. Total length of images 8 s and total height 245 μm. *C*: Typical records of spatially average Ca^{2+} transients shown as normalized fluo-3 fluorescence. Note that the transient was smaller and slower in the *ob/ob* cell. WT, wild-type.

RESEARCH DESIGN AND METHODS

Human insulin was from Novo Nordisk. The membrane permeable acetoxymethyl ester forms of fluo-3 and rhod-2 were from Molecular Probes. 2-aminoethoxydiphenyl borate (2-APB), wortmannin, and laminin were from Sigma. A membrane-permeable acetoxymethyl form of IP$_3$ (2,4,6-tri-*O*-butyryl-I[1,3,5]P$_3$) was obtained from Calbiochem. This IP$_3$ analog is more resistant to hydrolysis and metabolic degradation than the endogenous I(1,4,5)P$_3$, but the specificity is uncertain since I(1,3,5)P$_3$ itself has little affinity for the IP$_3$ receptor, which indicates that the phosphate groups of the analog can migrate to other positions in the inositol molecule (28). All compounds were prepared as stock solutions in appropriate solvents. On the day of the experiment, stock solutions were diluted to the desired final concentration in the bath solution; when required, the same concentration of solvent was added to the control solution.

Animal model and cell isolation. Young (3–5 months) C57BL genetically obese male mice (*ob/ob*; body weight 49.7 ± 2.6 g) and their wild-type counterparts (body weight 27.0 ± 1.1 g) were housed at room temperature with free access to standard food pellets and water. *Ob/ob* mice are profoundly hyperinsulinemic and display moderate increases in serum glucose and lipids (27). To ascertain that our *ob/ob* mice were insulin resistant, we measured the insulin-mediated 2-deoxyglucose uptake in isolated extensor digitorum longus muscles (29) and found a significantly lower rate of uptake in *ob/ob* compared with wild-type muscles (90 ± 6 vs. 130 ± 5 μmol · l^{-1} · min^{-1}, $n = 8$). One mouse was killed in the morning (~9:00 A.M.) of each experimental day by rapid neck disarticulation, and the heart was excised. Single cardiomyocytes were isolated from the ventricles following the protocols developed by the Alliance for Cellular Signaling (Procedure Protocol ID PP00000 125) (30). All experiments were approved by the Stockholm North local ethical committee.

Measurement of cytosolic Ca^{2+}. The free cytosolic [Ca^{2+}] was measured with the fluorescent Ca^{2+} indicator fluo-3. Isolated cardiomyocytes were incubated in Dulbecco's modified Eagle's medium (Sigma) containing 20 μmol/l fluo-3 AM for 40 min at room temperature followed by 10 min in medium without fluo-3. After being loaded, cardiomyocytes were plated on laminin-coated glass coverslips that made up the bottom of the perfusion chamber. Cells were superfused with standard Tyrode solution (mmol/l): 121 NaCl, 5.0 KCl, 1.8 CaCl$_2$, 0.5 MgCl$_2$, 0.4 NaH$_2$PO$_4$, 24 NaHCO$_3$, 0.1 EDTA, and 5.5 glucose. The solution was bubbled with 5% CO$_2$/95% O$_2$, which gives a bath pH of 7.4. Experiments were performed at room temperature (~24°C). Cells were stimulated with 1- to 2-ms current pulses delivered via two platinum electrodes (one on each side of the perfusion chamber). Changes in fluo-3 fluorescence were measured with confocal microscopy using a BioRad MRC 1024 unit (BioRad Microscopy Division, Hertfordshire, U.K.) attached to a Nikon Diaphot 200 inverted microscope with a Nikon Plan Apo 40× oil immersion objective (numerical aperture 1.3). Experiments were performed in the line-scan mode (6-ms intervals), and scanning was performed along the long axis of the cell. Excitation was at 488 nm, and the emitted light was collected through a 522-nm narrow band filter. The laser power used (3–6% of the maximum) did not have any noticeable deleterious effect on the fluorescent signal or cell function over the time course of an experiment. To enable comparisons between cells, changes in the fluorescence signal (ΔF) were divided by the fluorescence immediately before the stimulation pulse at 1-Hz stimulation (F_0). The time course of Ca^{2+} transients was assessed by measuring the time to peak (TTP); the half-width ($D_{1/2}$), i.e., the duration at 50% of ΔF; and the time constant (τ) of the exponential part of the decay phase, ignoring the initial decline that clearly diverged from a mono-exponential function (e.g., see wild-type transient in Fig. 1*C*).

Measurements of mitochondrial Ca^{2+}. Rhod-2 was used to measure mitochondrial Ca^{2+} (31). Isolated cardiomyocytes were loaded with rhod-2 AM (10 μmol/l) for 30 min at 4°C followed by washout and at least 1 h rest at room temperature. During the last 30 min of this rest period, cells were also loaded with fluo-3 AM (10 μmol/l) for 20 min followed by 10-min washout. Cells were continuously stimulated at 1 Hz, ensuring stable mitochondrial Ca^{2+} transients (31). Fluo-3 and rhod-2 fluorescence signals were obtained in the same line scan by excitation at 488 and 568 nm and measuring the emitted light at 522 and 585 nm, respectively. The fluo-3 signal was then used to subtract the cytosolic component of the rhod-2 signal leaving only the mitochondrial component. Control experiments were performed on wild-type cardiomyocytes where cells were only loaded with rhod-2 AM for 1 h at 4°C followed by at least 1 h washout at room temperature, a procedure that has been found to optimize mitochondrial rhod-2 loading in cardiomyocytes (31). These two procedures to assess mitochondrial Ca^{2+} gave very similar results that differed significantly ($P < 0.05$) from the cytosolic fluo-3 signals: under control conditions, the amplitude ($\Delta F/F_0$) was 3.1 ± 0.9 for the cytosolic fluo-3 signal vs. 1.8 ± 0.5 ($n = 12$) and 1.9 ± 0.6 ($n = 8$) for the mitochondrial fluo-3-subtracted and rhod-2 only signals, respectively; the time to peak was 25 ± 3 ms with fluo-3 vs. 115 ± 21 and 121 ± 20 ms in the two sets of rhod-2 measurements.

Measurements of IP$_3$. Cells were incubated in medium containing 10 mmol/l LiCl$_2$ in the absence or presence of insulin (60 nmol/l) for 15 min at room temperature. During the last 5 min, cells were allowed to settle at the bottom of the incubation tubes. The medium was removed and ice-cold 0.5 mol/l perchloric acid was added to the cells. The mixture was vortexed and kept in an ice slurry for 20 min. Thereafter, the acid extract was centrifuged (10,000*g* at 4°C for 15 min). The pellet was extracted with 1 mol/l NaOH for subsequent analysis of protein (Bio-Rad method). The supernatant was neutralized with ice-cold 2.2 mol/l KHCO$_3$ and centrifuged again. The final supernatant was analyzed for IP$_3$ using the [^{3}H] Biotrak Assay System (Amersham Biosciences, Piscataway, NJ).

Immunoprecipitation and Western blot analyses. Frozen hearts were thawed and left ventricles homogenized in lysis buffer comprising 20 mmol/l HEPES, pH 7.6, 150 mmol/l NaCl, 20% glycerol (vol/vol), 5 mmol/l EDTA, 1 mmol/l Na$_3$V0$_4$, 25 mmol/l KF, 0.5% Triton X-100 (vol/vol), and protease inhibitor cocktail (Roche). Lysates were cleared by centrifugation at 10,000*g* for 10 min at 4°C. The protein content was determined using the Bradford method (BioRad). Equal amounts of protein were incubated with primary antibodies for 5 min at room temperature, followed by addition of 30 μl of protein G agarose suspension (Santa Cruz Biotechnology, Santa Cruz, CA) for at least 4 h at 4°C with rotation. Primary antibodies used were anti-IP$_3$ receptor type 1 (anti-IP$_3$R1; gift from K. Rietdorf, L. Roderick, and M. Bootman

TABLE 1
Ca^{2+} transient characteristics

	n	$\Delta F/F_0$	TTP (ms)	$D_{1/2}$ (ms)	τ (ms)
Wild-type mice					
Control	33	3.6 ± 0.3	27.9 ± 3.8	167 ± 11	36.1 ± 2.9
Insulin (60 nmol/l)	15	4.6 ± 0.3*	26.0 ± 2.7	175 ± 8	37.1 ± 2.6
+ Wortmannin (0.5 μmol/l)	6	3.7 ± 0.5	29.0 ± 2.3	167 ± 5	37.7 ± 3.1
IP_3 (10 μmol/l)	18	3.8 ± 0.5	42.0 ± 4.1*	211 ± 12*	39.6 ± 4.1
Ob/ob mice					
Control	21	2.5 ± 0.3†	23.1 ± 2.1	189 ± 10†	46.8 ± 2.9†
Insulin (60 nmol/l)	18	2.7 ± 0.4†	50.3 ± 6.8*†	240 ± 13*†	39.1 ± 3.6
+ Wortmannin (0.5 μmol/l)	5	2.4 ± 1.1†	30.1 ± 7.4	194 ± 9†	47.5 ± 3.9†
IP_3 (10 μmol/l)	13	3.2 ± 0.2	61.2 ± 9.6*†	284 ± 27*†	40.2 ± 4.1

Data are means ± SE. $^*P < 0.05$ vs. the basal condition within each group (wild-type or *ob/ob*); $^†P < 0.05$, *ob/ob* vs. wild-type when studied under the same conditions. $\Delta F/F_0$, peak amplitude; TTP, time to peak; $D_{1/2}$, half-width; τ, decay time constant.

at the Babraham Institute, Cambridge, U.K.) and anti-IP_3 receptor type 2 (anti-IP_3R2; Santa Cruz). After washing three times with lysis buffer, samples were heated with SDS-PAGE sample buffer for 10 min at 70°C and proteins separated by 3–8% Tris-acetate gradient gels (Invitrogen) and transferred onto a polyvinylidine fluoride membrane (BioRad). Membranes were blocked in 5% (wt/vol) nonfat milk in Tris-buffered saline containing 0.05% Tween 20 followed by incubation with primary antibodies (anti-IP3R1, 1:6,000 dilution; anti-IP3R2, 1:100 dilution). Blots were then incubated with secondary horseradish peroxidase–conjugated antibody (anti-rabbit Ig, 1:40,000 [Amersham]; anti-goat Ig, 1:5,000 [BioRad]), and immunoreactive bands were visualized using enhanced chemiluminescence (SuperSignal; Pierce Biotechnology, Rockford, IL).

Statistics. Stored confocal images were analyzed with ImageJ (National Institutes of Health [available at http://rsb.info.nih.gov/ij/]). Data are presented as mean ± SE. Statistics were performed using Student's *t* test (for paired or unpaired samples) and one-way ANOVA when three or more groups were compared, along with a Newman-Keuls post hoc test. Differences were considered significant when the *P* value was <0.05.

RESULTS

Effects of insulin on cytoplasmic Ca^{2+} transients. We investigated characteristics of Ca^{2+} transients recorded during 1-Hz stimulation in wild-type and *ob/ob* mouse ventricular cardiomyocytes. Under control conditions, the amplitude of Ca^{2+} transients was smaller and the decay phase was slower in *ob/ob* compared with wild-type cardiomyocytes (Fig. 1). Contractions were also markedly weaker in *ob/ob* cells that shortened by 7.1 ± 0.8% of their resting length ($n = 21$) compared with 15.5 ± 1.8% ($n = 33$) in wild-type cells. Application of insulin (60 nmol/l = 10 mU/ml) significantly increased the Ca^{2+} transient amplitude by ~30% in wild-type cells, whereas there was no significant effect on the time course (Table 1). In *ob/ob* cardiomyocytes, on the other hand, insulin did not produce any significant change of the Ca^{2+} transient amplitude, but the transient became broader. This broadening of the transient was due to an increased time to peak and slowed onset of the decay phase, whereas the rate of decline during the final phase, if anything, tended to be faster in the presence of insulin (Table 1). Application of insulin triggered frequent extra Ca^{2+} transients during the final part of the decay phase in 10 of 18 *ob/ob* cardiomyocytes (Fig. 2). Such extra Ca^{2+} transients were not observed under control conditions in *ob/ob* cells, nor were they seen in wild-type cells even in the presence of insulin. Inhibition of PI3K with wortmannin (0.5 μmol/l) completely blocked the effects of insulin on Ca^{2+} transients in both wild-type and *ob/ob* cells (Table 1), which suggests that the effects of insulin occurred via the PI3K-dependent signaling pathway (10,11).

The concentration of insulin used in the experiments described above (60 nmol/l) is higher than that observed in vivo. We therefore also tested the effects of 6 nmol/l insulin, which is in the same range as the serum concentration of fed *ob/ob* mice (1.6 nmol/l) (27). The effects of 6 nmol/l insulin on Ca^{2+} transients were qualitatively the same as those observed with 60 nmol/l in both wild-type and *ob/ob* cells. Thus, in wild-type cardiomyocytes ($n = 5$), the peak amplitude of the Ca^{2+} transient increased from 3.5 ±. 0.2 in control to 4.1 ± 0.2 with 6 nmol/l insulin ($P < 0.05$), whereas the time to peak, half width, and decay time constant of the transient were not affected. In *ob/ob* cells ($n = 5$), application of 6 nmol/l insulin increased ($P < 0.05$) the time to peak (21.8 ± 2.9 ms in control vs. 42.0 ± 6.4 ms with insulin) and the half width (194 ± 12 vs. 209 ± 7 ms), whereas the peak amplitude and the decay time constant were not altered.

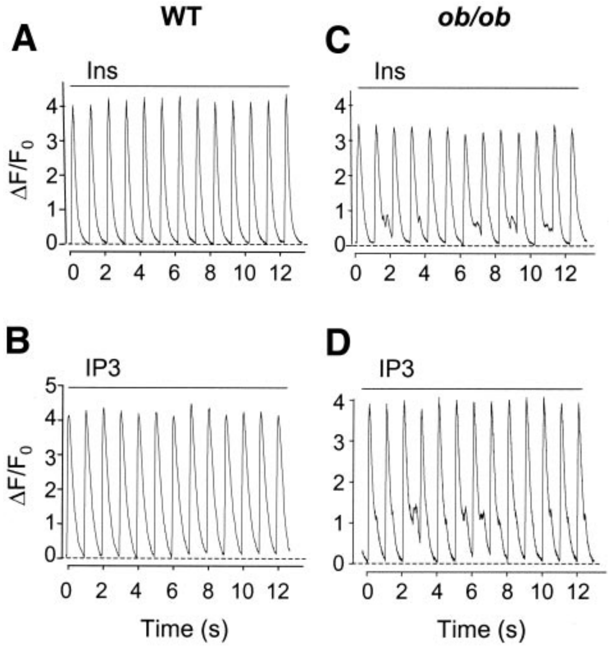

FIG. 2. Spatially averaged Ca^{2+} transients (expressed as normalized fluo-3 fluorescence) from a wild-type (WT; *A* and *B*) and an *ob/ob* (*C* and *D*) cell. Upper part (*A* and *C*) shows transients in the presence of insulin (Ins; 60 nmol/l) and lower part (*B* and *D*) after addition of a membrane-permeant IP_3 analog (IP3; 10 μmol/l). Note that frequent extra Ca^{2+} transients were triggered by insulin and IP_3 in the *ob/ob* cell.

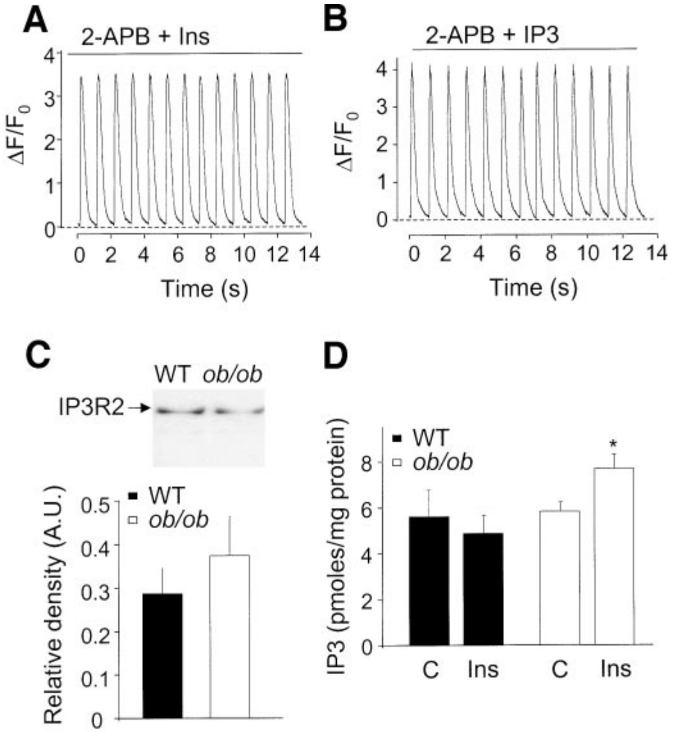

FIG. 3. Spatially averaged Ca^{2+} transients from an *ob/ob* cell recorded in the presence of 2-APB (30 μmol/l) and insulin (60 nmol/l) (*A*) or a membrane-permeant IP_3 analog (10 μmol/l) (*B*). Note that these compounds did not induce any extra Ca^{2+} transients in the presence of 2-APB. *C*: Representative immunoblots of IP_3 receptor type 2 in a wild-type and an *ob/ob* ventricle (*top*) and mean data (±SE) from six hearts (*bottom*). *D*: Mean data (n = 4–6 experiments) of the IP_3 concentration in wild-type (WT) and *ob/ob* cardiomyocytes under control conditions (C) and in the presence of insulin (Ins). *Significant difference ($P < 0.05$) between control and insulin.

Effects of IP_3 on cytoplasmic Ca^{2+} transients. We also tested the effect of a membrane-permeant IP_3 analog (10 μmol/l) on Ca^{2+} transients. Application of the IP_3 analog had no significant effect on the amplitude of Ca^{2+} transients in *ob/ob* or wild-type cardiomyocytes (Table 1). However, it produced broader Ca^{2+} transients in both groups due to an increased time to peak and slowed early decay phase, whereas the rate of the final decay was not affected. Moreover, the IP_3 analog induced extra Ca^{2+} transients in 8 of 13 *ob/ob* cells, whereas only 2 of 18 wild-type cells showed such transients (Fig. 2*B* and *D*).

To further investigate the possible role of IP_3 in insulin signaling, cells were preincubated for 15 min with 2-APB (30 μmol/l), a frequently used inhibitor of IP_3 receptors. 2-APB prevented the insulin-mediated slowing of the Ca^{2+} transient in *ob/ob* cells; for instance, in the presence of 2-APB, the time to peak was 28.6 ± 4.0 ms (n = 15) without and 33.2 ± 6.0 ms (n = 8) with insulin ($P > 0.05$, unpaired t test). Furthermore, no extra Ca^{2+} transients were triggered by insulin in the presence of 2-APB (Fig. 3*A*). 2-APB also prevented the IP_3-mediated slowing of the Ca^{2+} transient (time to peak 34.3 ± 7.4 ms [n = 7]) and prevented the induction of extra Ca^{2+} transients in *ob/ob* cells (Fig. 3*B*). However, 2-APB did not inhibit the insulin-induced increase in the Ca^{2+} transient amplitude in wild-type cells: $\Delta F/F_0$ was 3.1 ± 0.5 without and 4.0 ± 0.3 with insulin, respectively (n = 7).

Expression of IP_3 receptors and insulin effects on the IP_3 concentration. We used immunoprecipitation and

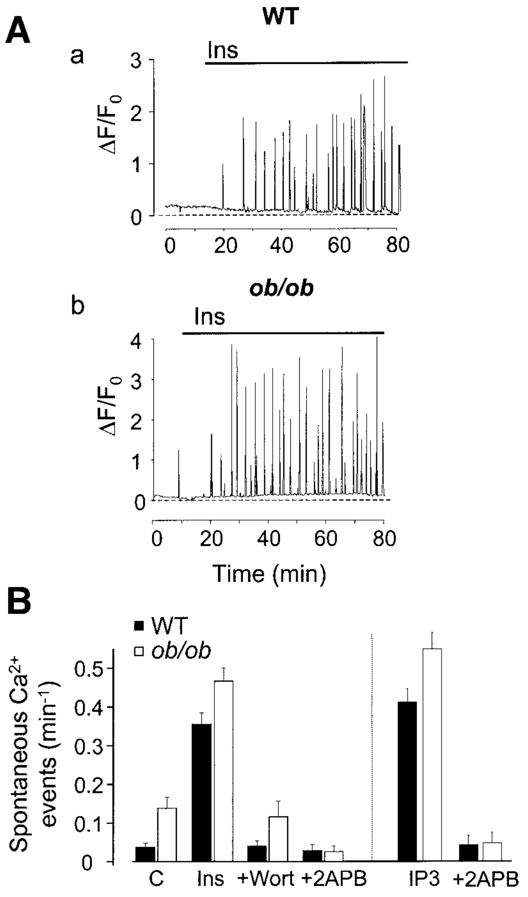

FIG. 4. *A*: Ca^{2+} records from a rested (not paced) cardiomyocyte of a wild-type (*a*) and an *ob/ob* (*b*) mouse. Note that insulin (60 nmol/l) induced frequent spontaneous Ca^{2+} events in both cells. *B*: Mean data (±SE) of the frequency of spontaneous Ca^{2+} events under control conditions (C) and in the presence of insulin (Ins) plus wortmannin (0.5 μmol/l; +Wort) or 2-APB (30 μmol/l; +2APB). Mean data from IP_3 (IP3) and +2-APB–exposed cardiomyocytes are also shown. Data from at least seven cells in each group. WT, wild-type.

Western blots to measure the expression of IP_3 receptor type 1 and type 2 in ventricles from wild-type and *ob/ob* mice, of which type 2 is the predominant isoform in cardiomyocytes (32). The mean expression of IP_3 receptor type 2 was not different between *ob/ob* and wild-type ventricles (P = 0.41) (Fig. 3*C*). Moreover, there was no difference in the expression of IP_3 receptor type 1 (data not shown).

The IP_3 concentration was measured in wild-type and *ob/ob* cardiomyocytes in the absence and presence of insulin. Insulin had no effect on the IP_3 concentration in wild-type cells, whereas it significantly ($P < 0.05$) increased the concentration by ~30% in *ob/ob* cells (Fig. 3*D*).

Spontaneous Ca^{2+} waves. Since IP_3 has been shown to generate arrhythmias and spontaneous Ca^{2+} events in cardiomyocytes (17,19), we studied the occurrence of spontaneous propagating Ca^{2+} waves in resting (not paced) cardiomyocytes. Few spontaneous Ca^{2+} waves were observed under control conditions. Application of insulin (60 nmol/l) significantly increased the frequency of waves in both wild-type and *ob/ob* cells (Fig. 4*A*). The insulin-induced increase in the frequency of spontaneous waves was fully reversed after 15-min washout in both cell groups (data not shown). Pretreatment with wortmannin

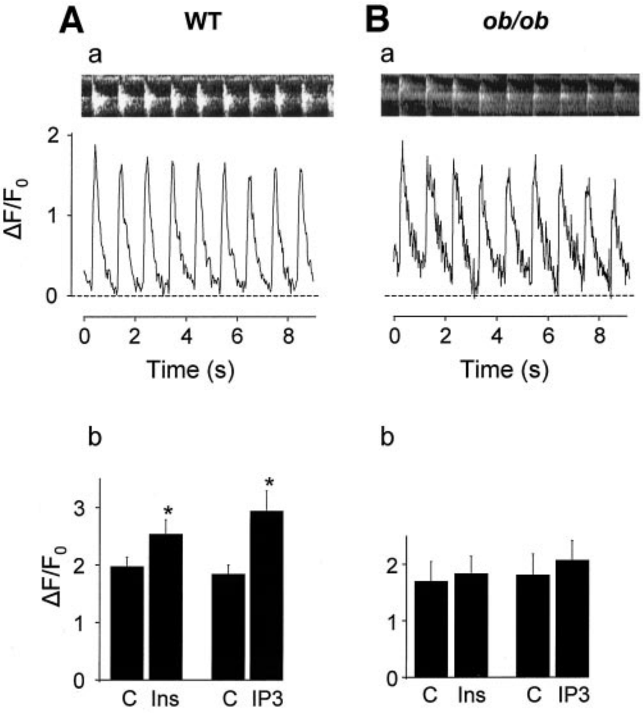

FIG. 5. Mitochondrial Ca^{2+} measured with rhod-2 in isolated wild-type (*A*) and *ob/ob* cardiomyocytes (*B*). *a*: Confocal line-scan images of areas rich in mitochondria during 1-Hz stimulation (*top*) and normalized rhod-2 fluorescence records (*bottom*). Height of line-scan images 20 μm. Note the markedly slower decay phase in the *ob/ob* cell. *b*: Mean data (±SE) of the normalized rhod-2 fluorescence amplitude under control conditions (C) and in the presence of insulin (Ins) or the IP_3 analog (IP3). *Statistical difference from control ($P < 0.05$). Data from at least six cells in each group.

or 2-APB completely blocked the insulin-mediated increase in wave frequency (Fig. 4*B*).

The effect of IP_3 was also tested under the same experimental conditions. IP_3 application resulted in frequent spontaneous propagating Ca^{2+} waves, and the effect was completely blocked by 2-APB (Fig. 4*B*).

Mitochondrial Ca^{2+} transient. Insulin had markedly different effects on cytosolic Ca^{2+} transients in wild-type and *ob/ob* cardiomyocytes, producing an increase in the amplitude in wild-type cells, whereas Ca^{2+} transients were broadened and extra transients occured during relaxation in *ob/ob* cells (see Table 1 and Fig. 2). Altered mitochondrial Ca^{2+} uptake in a beat-to-beat manner may have a role in this difference between wild-type and *ob/ob* cardiomyocytes, since mitochondria are known to contribute to the shaping of Ca^{2+} signals in cardiomyocytes (33) and diabetes is associated with impaired mitochondrial function (27). We therefore recorded transients of mitochondrial rhod-2 fluorescence at 1-Hz stimulation in the absence or presence of insulin (60 nmol/l). There was no difference between wild-type and *ob/ob* cells regarding the amplitude of mitochondrial Ca^{2+} transients under control conditions. However, the transients were significantly ($P < 0.05$) slower in *ob/ob* compared with wild-type cells (Fig. 5, *top*), with the time to peak and half-width being 182 ± 19 and 325 ± 24 ms in *ob/ob* cells ($n = 14$) vs. 115 ± 21 and 222 ± 20 ms in wild-type cells ($n = 12$), respectively. Application of insulin significantly increased the amplitude of mitochondrial Ca^{2+} transients in wild-type cells, whereas the amplitude was not changed in *ob/ob* cells (Fig. 5, *bottom*). Application of the IP_3 analog also increased the amplitude in wild-type but not in *ob/ob* cells. Thus, the dynamic mitochondrial Ca^{2+} buffering during insulin or IP_3 exposure was blunted in *ob/ob* cardiomyocytes.

DISCUSSION

Defects in the intracellular Ca^{2+} handling appear to be a generalized problem in diabetes (7). In the present study, we compared critical aspects of intracellular Ca^{2+} handling in ventricular cardiomyocytes of wild-type and *ob/ob* mice, a model of obesity and type 2 diabetes. The major novel results are *1*) insulin triggers extra Ca^{2+} transients in *ob/ob* but not in wild-type cardiomyocytes, which indicates an increased susceptibility for developing arrhythmias in *ob/ob* hearts; *2*) the effects of insulin on Ca^{2+} transients are reproduced by application of a membrane-permeant IP_3 analog in *ob/ob* but not in wild-type cardiomyocytes; *3*) in *ob/ob* cardiomyocytes, the effects of insulin and IP_3 were blocked by 2-APB, and insulin increased the IP_3 concentration; and *4*) mitochondrial Ca^{2+} handling was impaired in *ob/ob* cardiomyocytes.

Ca^{2+} transients in obesity and type 2 diabetes. Under control conditions, electrically evoked Ca^{2+} transients were smaller and slower in *ob/ob* cells, which may account for the decrease in peak contraction and slowed relaxation observed in different models of obesity and type 2 diabetes (34–36). Moreover, a recent study on cardiomyocytes isolated from obese, type 2 diabetic mice lacking functional leptin receptors (*db/db* mice) also showed significantly smaller and slower Ca^{2+} transients in comparison with control cells (37).

Ca^{2+} transients in cardiomyocytes are mediated by Ca^{2+} influx through voltage-activated L-type Ca^{2+} channels, which activate sarcoplasmic reticulum Ca^{2+} release channels (ryanodine receptor-2) via a process known as Ca^{2+}-induced Ca^{2+} release (38,39). Relaxation occurs when Ca^{2+} release is stopped and Ca^{2+} removed from the cytoplasm. This occurs predominantly by active reuptake into the sarcoplasmic reticulum by Ca^{2+} ATPase 2A, but Ca^{2+} extrusion out of the cell via Na^+/Ca^{2+} exchange also contributes (39). The Ca^{2+} transient amplitude increased when insulin was applied in wild-type but not in *ob/ob* cardiomyocytes. This difference might reflect an inability of insulin to increase the L-type Ca^{2+} current in type 2 diabetes, whereas the inotropic effect of insulin is at least partly attributable to an increased L-type Ca^{2+} current in normal subjects (40–42). This suggestion fits with our finding that 2-APB, which preferentially inhibits IP_3-mediated signaling (43), had no effect on the insulin-induced increase in Ca^{2+} transient amplitude in wild-type cells, whereas it blocked the effects of insulin on Ca^{2+} handling in *ob/ob* cells. Thus, the insulin-induced increase of the Ca^{2+} transient amplitude in wild-type cells appears not to be mediated via IP_3.

Possible role of IP_3 in the insulin signaling. Insulin application resulted in slowed Ca^{2+} transient kinetics and the appearance of frequent extra Ca^{2+} transients in *ob/ob* but not in wild-type cardiomyocytes. The insulin-mediated slowing of Ca^{2+} transients in *ob/ob* cells was due to an increased time to peak and slowed onset of the decay phase, whereas the rate of decline during the exponential decay phase was, if anything, increased (see Table 1). This indicates that insulin prolonged the sarcoplasmic reticulum Ca^{2+} release process whereas it had little effect on Ca^{2+} removal, which is dominated by the active sarcoplasmic reticulum Ca^{2+} reuptake (39). Application of a membrane-permeant IP$_3$ analog gave results qualitatively the same as those of insulin in *ob/ob* cells; that is, there was no significant effect on the Ca^{2+} transient amplitude or the exponential decay rate, whereas the time to peak was increased, the early decay phase was slowed, and frequent extra Ca^{2+} transients were produced. Thus, both insulin and IP$_3$ apparently increased the duration of action potential-mediated sarcoplasmic reticulum Ca^{2+} release in *ob/ob* cells, and this was accompanied by the triggering of extra Ca^{2+} transients. In accordance with these findings, insulin application caused an ~30% increase in the IP$_3$ concentration in *ob/ob* cardiomyocytes. On the other hand, the expression of type 1 and 2 IP$_3$ receptors was not different between *ob/ob* and wild-type ventricles, and hence this cannot explain the differences between the two groups regarding the response to insulin and IP$_3$.

The involvement of IP$_3$ in insulin signaling in cardiomyocytes is further supported by the fact that the insulin- and IP$_3$-mediated effects on electrically evoked Ca^{2+} transients in *ob/ob* cells were prevented by preincubation with 2-APB (see Fig. 3), one important action of which is to inhibit IP$_3$ receptors (43). Furthermore, both insulin and IP$_3$ induced spontaneous Ca^{2+} waves in rested wild-type and *ob/ob* cardiomyocytes, and this effect was fully blocked by 2-APB (Fig. 4). Finally, several studies have shown that IP$_3$ can induce cardiac arrhythmias (17–19), which fits with the occurrence of insulin- and IP$_3$-induced extra Ca^{2+} transients in *ob/ob* cells.

Possible role of defective mitochondrial function in impaired intracellular Ca^{2+} handling. An increase in mitochondrial Ca^{2+} may stimulate oxidative metabolism via activation of enzymes involved in mitochondrial energy production (44–46). Dynamic changes in mitochondrial Ca^{2+} are driven by the cytosolic Ca^{2+} transients in beating cardiomyocytes (31), thus providing a simple and elegant link between work and energy supply. Furthermore, a marked increase in mitochondrial Ca^{2+} in response to IP$_3$-linked stimuli has been observed in a large variety of cell types (47). In terms of regulating global cytosolic Ca^{2+} handling, mitochondria are believed to act as a spatial buffering system that can blunt or slow propagating Ca^{2+} waves (48,49), as well as directly controlling Ca^{2+} release via IP$_3$ receptors (49). Conversely, impaired mitochondrial Ca^{2+} accumulation may have deleterious effects by increasing cytosolic Ca^{2+} (49). In the present study, we showed slowed mitochondrial Ca^{2+} uptake in *ob/ob* cardiomyocytes compared with wild-type cells. Furthermore, the mitochondrial Ca^{2+} uptake did not increase in response to insulin or IP$_3$ in *ob/ob* cells. Thus, the impaired mitochondrial Ca^{2+} uptake in *ob/ob* cells may contribute to the larger slowing of Ca^{2+} transients induced by insulin and IP$_3$ in these cells, as well as the occurrence of extra Ca^{2+} transients.

We used rhod-2 to monitor mitochondrial Ca^{2+}, and although this nonratiometric dye can readily measure transient changes in Ca^{2+}, it is less suitable for detecting changes in basal mitochondrial Ca^{2+} accumulation. Thus, we are not able to distinguish between a basal mitochondrial Ca^{2+} overload or primary changes in mitochondrial Ca^{2+} flux kinetics as the major mechanism underlying the alterations observed in *ob/ob* cardiomyocytes.

Based on the present results, we propose the following model to explain the impaired Ca^{2+} handling in *ob/ob* cardiomyocytes: insulin increases the IP$_3$ concentration in *ob/ob* cardiomyocytes, which prolongs electrically evoked sarcoplasmic reticulum Ca^{2+} release. Mitochondrial Ca^{2+} uptake is impaired in *ob/ob* cardiomyocytes, which decreases the ability to buffer the extra Ca^{2+} released during physiological challenges. Together, these defects in *ob/ob* cardiomyocytes cause a slowing of the Ca^{2+} transient and increase the probability of extra Ca^{2+} transients that may predispose for arrhythmias in vivo.

ACKNOWLEDGMENTS

This study was supported by the Swedish Research Council (project numbers 10842 and 14453), the Swedish Heart and Lung Foundation, Biovitrum Partner Fund, the Swedish Diabetes Foundation, and Funds at the Karolinska Institutet.

REFERENCES

1. Eckel RH, Krauss RM: American Heart Association call to action: obesity as a major risk factor for coronary heart disease. AHA Nutrition Committee. *Circulation* 97:2099–2100, 1998
2. Kenchaiah S, Evans JC, Levy D, Wilson PW, Benjamin EJ, Larson MG, Kannel WB, Vasan RS: Obesity and the risk of heart failure. *N Engl J Med* 347:305–313, 2002
3. Bryant NJ, Govers R, James DE: Regulated transport of the glucose transporter GLUT4. *Nat Rev Mol Cell Biol* 3:267–277, 2002
4. Raman M, Nesto RW: Heart disease in diabetes mellitus. *Endocrinol Metab Clin North Am* 25:425–438, 1996
5. Chattou S, Diacono J, Feuvray D: Decrease in sodium-calcium exchange and calcium currents in diabetic rat ventricular myocytes. *Acta Physiol Scand* 166:137–144, 1999
6. Marra G, Cotroneo P, Pitocco D, Manto A, Di Leo MA, Ruotolo V, Caputo S, Giardina B, Ghirlanda G, Santini SA: Early increase of oxidative stress and reduced antioxidant defenses in patients with uncomplicated type 1 diabetes: a case for gender difference. *Diabetes Care* 25:370–375, 2002
7. Levy J: Abnormal cell calcium homeostasis in type 2 diabetes mellitus: a new look on old disease. *Endocrine* 10:1–6, 1999
8. Fang ZY, Prins JB, Marwick TH: Diabetic cardiomyopathy: evidence, mechanisms, and therapeutic implications. *Endocr Rev* 25:543–567, 2004
9. Brownsey RW, Boone AN, Allard MF: Actions of insulin on the mammalian heart: metabolism, pathology and biochemical mechanisms. *Cardiovasc Res* 34:3–24, 1997
10. Khan AH, Pessin JE: Insulin regulation of glucose uptake: a complex interplay of intracellular signalling pathways. *Diabetologia* 45:1475–1483, 2002
11. White MF: Insulin signaling in health and disease. *Science* 302:1710–1711, 2003
12. Bae YS, Cantley LG, Chen CS, Kim SR, Kwon KS, Rhee SG: Activation of phospholipase C-gamma by phosphatidylinositol 3,4,5-trisphosphate. *J Biol Chem* 273:4465–4469, 1998
13. Kayali AG, Eichhorn J, Haruta T, Morris AJ, Nelson JG, Vollenweider P, Olefsky JM, Webster NJ: Association of the insulin receptor with phospholipase C-gamma (PLCgamma) in 3T3–L1 adipocytes suggests a role for PLCgamma in metabolic signaling by insulin. *J Biol Chem* 273:13808–13818, 1998
14. Eichhorn J, Kayali AG, Austin DA, Webster NJ: Insulin activates phospholipase C-γ1 via a PI-3 kinase dependent mechanism in 3T3–L1 adipocytes. *Biochem Biophys Res Commun* 282:615–620, 2001
15. Kim MJ, Kim E, Ryu SH, Suh PG: The mechanism of phospholipase C-gamma1 regulation. *Exp Mol Med* 32:101–109, 2000
16. Kudoh A, Kudoh E, Katagai H, Takazawa T: Insulin potentiates bradykinin-induced inositol 1,4,5-triphosphate in neonatal rat cardiomyocytes. *J Cardiovasc Pharmacol* 39:621–627, 2002
17. Jacobsen AN, Du XJ, Lambert KA, Dart AM, Woodcock EA: Arrhythmogenic action of thrombin during myocardial reperfusion via release of inositol 1,4,5-triphosphate. *Circulation* 93:23–26, 1996

18. Zima AV, Blatter LA: Inositol-1,4,5-trisphosphate-dependent Ca^{2+} signalling in cat atrial excitation-contraction coupling and arrhythmias. *J Physiol* 555:607–615, 2004
19. Mackenzie L, Bootman MD, Laine M, Berridge MJ, Thuring J, Holmes A, Li WH, Lipp P: The role of inositol 1,4,5-trisphosphate receptors in Ca^{2+} signalling and the generation of arrhythmias in rat atrial myocytes. *J Physiol* 541:395–409, 2002
20. Putney JW Jr, Broad LM, Braun FJ, Lievremont JP, Bird GS: Mechanisms of capacitative calcium entry. *J Cell Sci* 114:2223–2229, 2001
21. Hunton DL, Lucchesi PA, Pang Y, Cheng X, Dell'Italia LJ, Marchase RB: Capacitative calcium entry contributes to nuclear factor of activated T-cells nuclear translocation and hypertrophy in cardiomyocytes. *J Biol Chem* 277:14266–14273, 2002
22. Pang Y, Hunton DL, Bounelis P, Marchase RB: Hyperglycemia inhibits capacitative calcium entry and hypertrophy in neonatal cardiomyocytes. *Diabetes* 51:3461–3467, 2002
23. Pang Y, Bounelis P, Chatham JC, Marchase RB: Hexosamine pathway is responsible for inhibition by diabetes of phenylephrine-induced inotropy. *Diabetes* 53:1074–1081, 2004
24. Brownlee M: Biochemistry and molecular cell biology of diabetic complications. *Nature* 414:813–820, 2001
25. Flarsheim CE, Grupp IL, Matlib MA: Mitochondrial dysfunction accompanies diastolic dysfunction in diabetic rat heart. *Am J Physiol* 271:H192–H202, 1996
26. Duchen MR: Roles of mitochondria in health and disease. *Diabetes* 53 (Suppl. 1):S96–S102, 2004
27. Mazumder PK, O'Neill BT, Roberts MW, Buchanan J, Yun UJ, Cooksey RC, Boudina S, Abel ED: Impaired cardiac efficiency and increased fatty acid oxidation in insulin-resistant ob/ob mouse hearts. *Diabetes* 53:2366–2374, 2004
28. Li WH, Schultz C, Llopis J, Tsien RY: Membrane-permeant esters of inositol polyphosphates, chemical syntheses and biological applications. *Tetrahedron* 53:12017–12040, 1997
29. Shashkin P, Koshkin A, Langley D, Ren JM, Westerblad H, Katz A: Effects of CGS 9343B (a putative calmodulin antagonist) on isolated skeletal muscle: dissociation of signaling pathways for insulin-mediated activation of glycogen synthase and hexose transport. *J Biol Chem* 270:25613–25618, 1995
30. Sambrano GR, Fraser I, Han H, Ni Y, O'Connell T, Yan Z, Stull JT: Navigating the signalling network in mouse cardiac myocytes. *Nature* 420:712–714, 2002
31. Trollinger DR, Cascio WE, Lemasters JJ: Selective loading of rhod 2 into mitochondria shows mitochondrial Ca^{2+} transients during the contractile cycle in adult rabbit cardiac myocytes. *Biochem J* 236:738–742, 1997
32. Lipp P, Laine M, Tovey SC, Burrell KM, Berridge MJ, Li W, Bootman MD: Functional InsP3 receptors that may modulate excitation-contraction coupling in the heart. *Curr Biol* 10:939–942, 2000
33. Mackenzie L, Roderick HL, Berridge MJ, Conway SJ, Bootman MD: The spatial pattern of atrial cardiomyocyte calcium signalling modulates contraction. *J Cell Sci* 117:6327–6337, 2004
34. Carroll JF, Jones AE, Hester RL, Reinhart GA, Cockrell K, Mizelle HL: Reduced cardiac contractile responsiveness to isoproterenol in obese rabbits. *Hypertension* 30:1376–1381, 1997
35. Ren J, Bode AM: Altered cardiac excitation-contraction coupling in ventricular myocytes from spontaneously diabetic BB rats. *Am J Physiol Heart Circ Physiol* 279:H238–H244, 2000
36. Christoffersen C, Bollano E, Lindegaard ML, Bartels ED, Goetze JP, Andersen CB, Nielsen LB: Cardiac lipid accumulation associated with diastolic dysfunction in obese mice. *Endocrinology* 144:3483–3490, 2003
37. Belke DD, Swanson EA, Dillmann WH: Decreased sarcoplasmic reticulum activity and contractility in diabetic *db/db* mouse heart. *Diabetes* 53:3201–3208, 2004
38. Fabiato A: Time and calcium dependence of activation and inactivation of calcium-induced release of calcium from the sarcoplasmic reticulum of a skinned canine cardiac Purkinje cell. *J Gen Physiol* 85:247–289, 1985
39. Bers DM: Sarcoplasmic reticulum Ca release in intact ventricular myocytes. *Front Biosci* 7:d1697–d1711, 2002
40. Aulbach F, Simm A, Maier S, Langenfeld H, Walter U, Kersting U, Kirstein M: Insulin stimulates the L-type Ca^{2+} current in rat cardiac myocytes. *Cardiovasc Res* 42:113–120, 1999
41. Maier S, Aulbach F, Simm A, Lange V, Langenfeld H, Behre H, Kersting U, Walter U, Kirstein M: Stimulation of L-type Ca^{2+} current in human atrial myocytes by insulin. *Cardiovasc Res* 44:390–397, 1999
42. Maier S, Lange V, Simm A, Walter U, Kirstein M: Insulin fails to modulate the cardiac L-type Ca^{2+} current in type II diabetes patients: a possible link to cardiac dysfunction in diabetes mellitus (Letter). *Diabetologia* 44:269, 2001
43. Peppiatt CM, Collins TJ, Mackenzie L, Conway SJ, Holmes AB, Bootman MD, Berridge MJ, Seo JT, Roderick HL: 2-Aminoethoxydiphenyl borate (2-APB) antagonises inositol 1,4,5-trisphosphate-induced calcium release, inhibits calcium pumps and has a use-dependent and slowly reversible action on store-operated calcium entry channels. *Cell Calcium* 34:97–108, 2003
44. Duchen MR: Ca^{2+}-dependent changes in the mitochondrial energetics in single dissociated mouse sensory neurons. *Biochem J* 283:41–50, 1992
45. Hajnoczky G, Csordas G, Krishnamurthy R, Szalai G: Mitochondrial calcium signaling driven by the IP3 receptor. *J Bioenerg Biomembr* 32:15–25, 2000
46. Duchen MR: Mitochondria in health and disease: perspectives on a new mitochondrial biology. *Mol Aspects Med* 25:365–451, 2004
47. Rizzuto R, Brini M, Murgia M, Pozzan T: Microdomains with high Ca^{2+} close to IP3-sensitive channels that are sensed by neighboring mitochondria. *Science* 262:744–747, 1993
48. Boitier E, Rea R, Duchen MR: Mitochondria exert a negative feedback on the propagation of intracellular Ca^{2+} waves in rat cortical astrocytes. *J Cell Biol* 145:795–808, 1999
49. Jaconi M, Bony C, Richards SM, Terzic A, Arnaudeau S, Vassort G, Puceat M: Inositol 1,4,5-trisphosphate directs Ca^{2+} flow between mitochondria and the endoplasmic/sarcoplasmic reticulum: a role in regulating cardiac autonomic Ca^{2+} spiking. *Mol Biol Cell* 11:1845–1858, 2000